PERGAMON

Deep-Sea Research II 49 (2002) 827–845

DEEP-SEA RESEARCH
PART II

www.elsevier.com/locate/dsr2

Viral distribution and activity in Antarctic waters

Núria Guixa-Boixereu, Dolors Vaqué, Josep M. Gasol, Jaime Sánchez-Cámara, Carlos Pedrós-Alió*

Departament de Biologia Marina i Oceanografia, Institut de Ciències del Mar (CMIMA, CSIC), Passeig Marítin de la Barceloneta, 37-49 E-08003 Barcelona, Spain

Received 5 October 1999; received in revised form 8 September 2000; accepted 6 June 2001

Abstract

Variability in abundance of virus-like particles (VLP), VLP decay rates and prokaryotic mortality due to viral infection were determined in three Antarctic areas: Bellingshausen Sea, Bransfield Strait and Gerlache Strait, during December 1995 and February 1996. VLP abundance showed very small spatial variability in the three areas (7×10^6–2×10^7 VLP ml^{-1}). VLP abundance, on the other hand, decreased one order of magnitude from the surface to the bottom, in two stations where deep vertical profiles were sampled. Low seasonal variability in VLP abundance was found when comparing each area separately. Diel VLP variability was also very low. VLP abundance showed the lowest values when solar irradiation was maximal, in two of the three stations where diel cycles were examined. Viral decay rates (VDR) were determined using KCN in two kinds of experiments. Type 1 experiments were performed in 6 stations to determine viral decay. Type 2 experiments were carried out in 2 stations to examine the influence of temperature and organic matter concentration on viral decay. VDR was not influenced by these parameters. Prokaryotic mortality due to viral infection was always higher than that due to bacterivores in the stations where both factors of prokaryotic mortality were measured. Viral infection accounted for all the prokaryotic heterotrophic production in Bellingshausen Sea and Gerlache Strait and for half of the prokaryotic heterotrophic production in Bransfield Strait. These high values of prokaryotic mortality due to viral infection are difficult to reconcile in nature, and more work is necessary to determine the mechanisms involved in the disappearance of viruses.

1. Introduction

Viruses have been shown to be present in high abundance and to account for a significant percentage of the prokaryotic mortality in different temperate marine habitats (e.g., Proctor and Fuhrman, 1990; Steward et al., 1992; Maranger and Bird, 1995; Weinbauer and Peduzzi, 1995). However, little is known about viral distribution and activity in cold marine environments. Virus-like particles (VLP) have been counted in surface waters in Bellingshausen Sea (Smith et al., 1992) and in Arctic sea ice (Maranger et al., 1994). And more recently, Steward et al. (1996) have measured viral production in pelagic environments from the Arctic (Bering and Chukchi Seas). In the later study, viruses accounted for an important percentage of prokaryotic mortality in the most productive waters (Steward et al., 1996).

The study of the Southern Ocean has a special interest because a markedly seasonal phytoplankton bloom sustains the entire food web. This is

*Corresponding author. Tel.: +34-93-230-9500; fax: +34-93-230-9555.

E-mail address: cpedros@icm.csic.es (C. Pedrós-Alió).

0967-0645/01/$ - see front matter
PII: S0967-0645(01)00126-6

particularly true for coastal ecosystems, where a large variation in rates of primary production exists throughout the year (Karl, 1993). The coastal shelf region between the Bransfield Strait and the Bellingshausen Sea is thought to be specially important because it supports an extensive spring bloom of phytoplankton and is a nursery area for Antarctic krill (Karl, 1993).

The only interdisciplinary study of microbiological processes in this area was conducted by the RACER program from December 1986 to March 1987, and later in October and November 1989 (Karl, 1993), although bacterivory and viral activity were not measured. An uncoupling between autotrophic and heterotrophic processes was observed (Bird and Karl, 1991). This uncoupling is claimed to be a general characteristic of high-latitude oceans (Pomeroy and Deibel, 1986; Karl, 1993).

The mechanisms responsible for the apparent suppression of the microbial activity in the first stages of the phytoplankton bloom are not well understood. It has been suggested that low temperature could have differential effects on the different components of the microbial plankton (Pomeroy and Deibel, 1986). At the same time, other components of the microbial loop that have been shown to control prokaryotic activity and abundance in more temperate latitudes are not well documented in Antarctic waters. Few data are available about protozoan grazing (Vaqué et al., 2002) and, as pointed out before, the role of viruses is essentially unknown.

The goal of our work was to determine the variability in VLP abundance and dynamics in several representative habitats of this coastal region close to the Antarctic Peninsula (southern Bellingshausen Sea, western Bransfield Strait and Gerlache Strait) during the austral spring and summer. First, we described the spatial and temporal distribution of VLP abundance in the region. Second, we measured viral decay in some representative stations and used this parameter as an indicator of viral activity. We also investigated the influence of organic matter and temperature on viral decay rates and the abiotic factors responsible for viral decay. Finally, we calculated prokaryotic mortality due to viral infection and compared its importance to protozoan bacterivory.

2. Material and methods

2.1. Study area and sampling

Samples were collected during two cruises on board the BIO *Hespérides* from December 1995 to January 1996 (FRUELA 95) and from January to February 1996 (FRUELA 96). This period of time corresponded to late spring and summer. The area studied (Fig. 1) included several representative Antarctic waters: (1) two different deep-water zones (the western basin of the Bransfield Strait and the eastern Bellingshausen Sea); (2) a frontal zone between the Bellingshausen Sea and Bransfield Strait water masses and (3) the eutrophic and

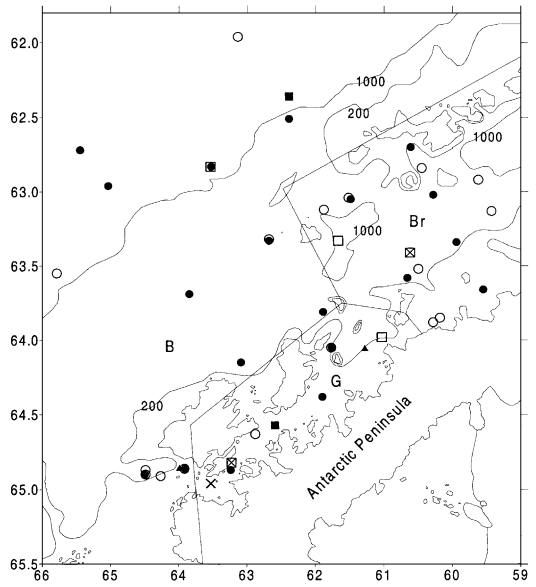

Fig. 1. Study area in the eastern Bellingshausen Sea (B), Bransfield (Br) and Gerlache (G) Straits with location of the stations used for VLP counts: shallow vertical profiles (circles), deep vertical profiles (triangles), diel cycles (crosses) and decay rate experiments (squares). Empty symbols indicate stations sampled during FRUELA 95 and full symbols during FRUELA 96. Depth is in meters.

mesotrophic coastal region of Gerlache Strait. Seawater samples for depth profiles and diel cycles were collected with 12-l Niskin bottles mounted on a rosette with a Mark II CTD. Details about the water circulation in the area can be found in Gomis et al. (2002).

2.2. Abundance of microorganisms

Chlorophyll *a* was measured by fluorometry in acetone extracts (Yentsch and Menzel, 1963). Between 25 and 200 ml^{-1} of seawater was filtered through GF/F filters. The filters were subsequently stored for 24 h in 90% acetone. Fluorescence of the chlorophyll extracts was determined with a Turner Designs fluorometer.

Samples for prokaryotic counting were preserved in 2% glutaraldehyde and stored in polypropylene bottles until they could be processed. Bacteria were stained with DAPI (1 $\mu g\,ml^{-1}$ final concentration) and filtered onto black 0.2-μm pore size polycarbonate filters (Porter and Feig, 1980) on board, mounted on microscopy slides, and frozen. Prokaryotic abundance was determined with a Nikon epifluorescence microscopy at a magnification of $1250\times$.

Samples for VLP counting were immediately filtered and stained with YO-PRO 1 (Hennes and Suttle, 1995). The stock solution of YO-PRO 1 (1 mM in a 1 : 4 solution of dimethyl sulfoxide and water) was diluted to 50 μM in an aqueous solution of 2 mM KCN. 100 μl of unfixed sample was diluted with 700 μl of mili Q water filtered through a 0.02-μm pore size filter (Anodisc). Each diluted sample was gently filtered through a 0.02 μm pore size Anodisc 25 filter. The Anodisc filter with the filtered sample was laid on 80 μl of the staining solution in a Petri dish and incubated in the dark for two days at room temperature. The filters were then washed twice by filtering 800 μl of mili Q water through the membrane. Filters were transferred to glass slides, immediately covered with a drop of spectrophotometric-grade glycerol and a cover slip. Filters were stored at $-20^{\circ}C$ until counted. VLP abundance was determined with a Nikon epifluorescence microscopy at a magnification of $1250\times$.

2.3. Prokaryotic heterotrophic production

Prokaryotic heterotrophic production was determined by ^{3}H-leucine incorporation (Kirchman et al., 1985) as modified for micro-centrifugation by Smith and Azam (1992). Four replicates and two controls killed with trichloroacetic acid (TCA, 5% final concentration) for each sample were incubated in the dark, at in situ temperature, with 20 nM Leu in 2 ml capacity microcentrifuge tubes. Incubations were terminated by addition of TCA (5% final concentration) after 4 h. The tubes were centrifuged for 10 min at 16,000*g* and the supernatant aspirated. The samples were washed by the addition of 1.5 ml of 5% TCA and vortex mixing. Samples were centrifuged again (10 min, 16,000*g*) and aspirated. ^{3}H-leucine incorporated was converted to carbon produced using an empirically determined conversion factor estimated for the area of 0.86 kg C mol $leucine^{-1}$ (Pedrós-Alió et al., 2002). In order to calculate viral impact on prokaryotic heterotrophic production, carbon produced was converted to cells produced. For this purpose carbon content per cell was estimated substituting an average prokaryotic volume of 0.07 μm^3 (Calderón-Paz, 1997) in the equation $pg\,C = 0.09\,(\mu m^3)^{0.9}$ (Norland et al., 1987).

2.4. Viral decay rates

Water samples for these determinations were collected from representative stations in the three areas sampled: Gerlache Strait, Bransfield Strait and Bellingshausen Sea (Table 1; Fig. 1). All incubations were made in polyethylene bottles in the dark. Different volumes (from 100 ml to 1 l) were used in different experiments. Previously, we had checked that the different volumes used did not influence the rate of viral decay obtained. Viral decay rate was recorded after inhibiting production of new viruses by adding KCN to a final concentration of 2 mM (Heldal and Bratbak, 1991). Samples for ^{3}H-leucine incorporation were taken at the beginning and at the end of each experiment in order to confirm that the prokaryotic activity had been inhibited by the KCN. The viral decay rate (VDR) was calculated from the log-linear part of the decay curves using linear

Table 1
Date and location of the stations with the integrated values (from surface to 80–100 m) of prokaryotic (PN) and VLP abundance, VLP/PN ratio and chlorophyll *a*

Station	Date (d/m/y)	Latitude S	Longitude W	PN (l^{-1})	VLP (l^{-1})	VLP/PN	Chlorophyll ($\mu g\, l^{-1}$)
(A) *Stations sampled in FRUELA 95*							
5	4/12/95	63° 51′ 06″	60° 10′ 37″	3.44×10^8	1.14×10^{10}	33.21	0.74
8	4/12/95	63° 02′ 32″	61° 30′ 55″	4.85×10^8	9.17×10^9	18.88	0.73
12	5/12/95	61° 57′ 51″	63° 08′ 29″	2.33×10^8	1.05×10^{10}	45.23	2.09
15	6/12/95	62° 49′ 30″	63° 32′ 13″	2.87×10^8	2.33×10^{10}	81.42	3.57
17	6/12/95	63° 19′ 29″	62° 41′ 00″	3.94×10^8	1.83×10^{10}	46.46	1.08
29	8/12/95	63° 33′ 03″	65° 47′ 26″	2.32×10^8	8.20×10^9	35.32	2.83
34	9/12/95	64° 54′ 06″	64° 29′ 20″	1.82×10^8	1.23×10^{10}	67.61	1.60
39	10/12/95	64° 52′ 01″	64° 29′ 20″	2.55×10^8	1.41×10^{10}	55.29	1.94
40	10/12/95	64° 37′ 50″	62° 52′ 54″	3.06×10^8	1.75×10^{10}	57.23	3.43
47	11/12/95	64° 03′ 09″	61° 46′ 03″	4.64×10^8	1.41×10^{10}	30.40	2.28
72	13/12/95	63° 58′ 31″	61° 01′ 39″	4.58×10^8	1.10×10^{10}	24.12	1.12
79	14/12/95	63° 19′ 54″	61° 40′ 23″	3.40×10^8	1.29×10^{10}	38.00	0.63
81	14/12/95	63° 07′ 17″	61° 52′ 59″	6.03×10^8	2.01×10^{10}	33.35	0.85
94	15/12/95	63° 52′ 34″	60° 16′ 33″	3.97×10^8	1.47×10^{10}	36.93	
97	15/12/95	63° 31′ 21″	60° 30′ 00″	3.67×10^8	1.00×10^{10}	27.29	0.89
123	17/12/95	62° 50′ 22″	60° 26′ 57″	4.90×10^8	9.92×10^9	20.24	0.53
140	18/12/95	63° 07′ 49″	59° 25′ 31″	3.90×10^8	1.42×10^{10}	36.42	1.78
142	18/12/95	62° 55′ 03″	59° 37′ 14″	4.95×10^8	1.30×10^{10}	26.15	0.91
37	20/12/95	64° 51′ 27″	63° 54′ 59″	3.86×10^8	1.21×10^{10}	31.35	1.66
36	20/12/95	64° 54′ 20″	64° 15′ 56″	3.10×10^8	1.22×10^{10}	39.29	
156	21/12/95	64° 57′ 28″	63° 31′ 42″	1.76×10^8	1.02×10^{10}	58.08	1.93
168	26/12/95	63° 24′ 28″	60° 37′ 16″	3.36×10^8	1.56×10^{10}	30.55	1.63
169	28/12/95	64° 48′ 54″	63° 13′ 50″	5.18×10^8	2.20×10^{10}	42.63	2.82
(B) *Stations sampled in FRUELA 96*							
186	19/1/96	64° 03′ 11″	61° 45′ 46″	5.65×10^8	1.01×10^{10}	17.88	
187	191//96	64° 53′ 47″	64° 30′ 11″	5.88×10^8	1.04×10^9	17.69	1.49
189	20/1/96	64° 51′ 20″	63° 54′ 42″	7.76×10^8	1.08×10^{10}	13.99	2.28
191	20/1/96	64° 52′ 08″	63° 14′ 39″	5.90×10^8	1.09×10^{10}	18.56	4.22
193	20/1/96	64° 34′ 01″	62° 35′ 27″	5.72×10^8	1.12×10^{10}	19.64	2.24
195	21/1/96	64° 22′ 46″	61° 54′ 05″	4.65×10^8	1.08×10^9	23.27	1.07
197	21/1/96	62° 43′ 12″	65° 27′ 13″	4.25×10^8	1.01×10^{10}	23.78	0.07
198	22/1/96	62° 57′ 48″	65° 02′ 41″	3.22×10^8	1.39×10^{10}	26.58	0.23
200	24/1/96	63° 41′ 13″	63° 51′ 02″	2.78×10^8	7.64×10^9	27.53	0.38
203	23/1/96	64° 08′ 47″	63° 05′ 33″	3.22×10^8	1.39×10^{10}	43.03	0.39
204	23/1/96	63° 48′ 28″	61° 53′ 09″	3.60×10^8	1.40×10^{10}	38.33	0.46
206	23/1/96	63° 19′ 43″	62° 40′ 57″	2.69×10^8	1.33×10^{10}	49.57	0.32
208	24/1/96	62° 49′ 42″	63° 32′ 04″	2.23×10^8	7.12×10^9	31.96	0.11
210	24/1/96	62° 21′ 39″	62° 23′ 07″	3.19×10^8	1.03×10^9	32.26	
213	25/1/96	62° 30′ 20″	62° 23′ 07″	2.82×10^8	7.44×10^{10}	26.36	0.34
215	26/1/96	63° 02′ 43″	61° 29′ 36″	2.98×10^8	1.02×10^9	34.13	0.37
217	26/1/96	63° 34′ 37″	60° 39′ 25″	3.12×10^8	1.01×10^{10}	32.35	0.65
219	26/1/96	63° 39′ 26″	59° 32′ 50″	3.37×10^8	1.44×10^{10}	42.70	0.72
220	27/1/96	63° 20′ 12″	59° 56′ 22″	3.44×10^8	1.02×10^{10}	29.60	0.45
221	27/1/96	63° 01′ 01″	60° 16′ 40″	2.77×10^8	1.28×10^{10}	46.16	0.88
222	27/1/96	62° 41′ 49″	60° 36′ 27″	4.02×10^8	1.22×10^{10}	30.26	0.29
225	1/2/96	64° 03′ 39″	61° 17′ 01″	6.69×10^8	1.55×10^{10}	23.15	3.49
226	3/2/96	64° 51′ 30″	63° 59′ 17″	5.91×10^8	1.06×10^{10}	17.90	5.29

regression. Two types of experiments were carried out.

Type I experiments were designed to investigate viral decay rates. These experiments were done in three stations from Gerlache Strait (72, 169 and 193), two stations from Bransfield Strait (168 and 79) and two stations from Bellingshausen Sea (15 and 210; Fig. 1). Stations 15, 72, 79, 168 and 169 were occupied during FRUELA 95 and stations 193 and 210 during FRUELA 96 (Table 1; Fig 1). In each experiment, a 2-l sample was taken from 5 m deep water (20 m in station 15) and divided into two parts: 1 l was filtered through 0.8 μm polycarbonate filters and the other liter through 50 μm net filter. Decay rate experiments were carried out with the filtered samples as described before. The filtered water was incubated at in situ temperature after addition of KCN (inactive cultures). Samples for VLP counts were retrieved frequently (2–3 h) during the first 12 h and occasionally afterwards up to 48 h. Cyanide was added again after 24 h to insure an inhibiting concentration of KCN during FRUELA 95, but not in the two FRUELA 96 experiments. In some of these experiments (stations 15, 72 and 168) we had parallel incubations of water without cyanide (active cultures).

Type II experiments were carried out to examine the influence of temperature and organic matter concentration on viral decay. Eight liters of 5 m water from a station in Gerlache Strait (72; Table 1; Fig. 1) and a station in Bransfield Strait (168; Table 1; Fig. 1) was filtered through 0.8-μm polycarbonate filters to remove bacterivores. Filtered water was dispensed into 1 l, acid washed, autoclaved, Pyrex bottles. The resulting eight batch cultures were divided into two groups: one group received a glucose addition (10 μM final concentration) and the other was used as control. Each pair of batch cultures was incubated at four different temperatures: −1°C, 0°C, 4°C, 5°C (station 72) and −1°C, 0°C, 4°C, 8°C (station 168). Thus, for each temperature, we had two cultures: control and glucose addition. Samples for prokaryotic and VLP abundance and ^{3}H-leucine incorporation were taken every day during 5–6 days. On the third sampling day, viral decay rate experiments were performed with 100-ml aliquots from each batch culture as described before. The incubations for determining viral decay rates were done at the same temperature as the original batch cultures. In station 168 viral decay rate determinations were carried out only in the batch cultures incubated at −1°C and 8°C.

3. Results

3.1. Viral abundance and distribution

Vertical distribution of VLP and prokaryotic abundance were investigated from the surface to the bottom in stations 225 and 226 (Table 1; Figs. 1 and 2). Both VLP and prokaryotic abundance decreased with depth. The VLP/BN ratio was minimal (10/1) at the deepest points in both stations and maximal at the surface in station 225 (50/1) and at 200 m in station 226 (32.5/1).

Correlations between VLP and prokaryotic abundance and between VLP abundance and chlorophyll *a* were calculated with the data from all the stations and depths shown in Table 1. Significant correlations are shown in Table 2. These correlations also were calculated for each cruise (FRUELA 95 and 96) and for each area (Bellingshausen, Bransfield and Gerlache) separately. Correlations in Bransfield Strait and in Bellingshausen Sea were not different from those presented with the data of both cruises together. In all cases, prokaryotic abundance and chlorophyll explained less than 50% of the variability in VLP abundance.

Distribution of VLP abundance was compared among the three areas using the integrated values from surface to 80 or 100 m (Table 1; Fig. 1). VLP abundance was not significantly different among the three areas studied for any of the cruises (ANOVA, FRUELA 95, $p = 0.817$, $n = 20$, FRUELA 96, $p = 0.317$, $n = 23$; Fig. 3). For the VLP/BN ratio however, ANOVA revealed significant differences between the three areas investigated in FRUELA 96 ($p < 0.001$, $n = 22$). A post hoc Tukey test indicated that the significant differences were those between Gerlache Strait and the other areas ($p < 0.001$; Fig. 3). For the cruise

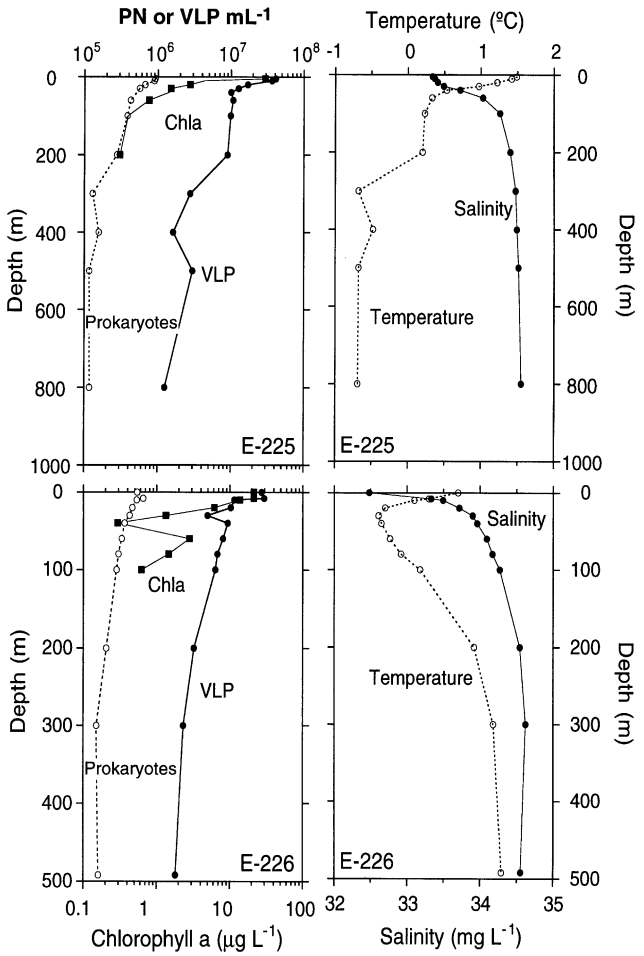

Fig. 2. Deep vertical profiles from stations 225 (upper panels) and 226 (lower panels) of temperature, salinity, chlorophyll *a* concentration, prokaryotic and VLP abundance.

Table 2
Correlation coefficients between VLP abundance and prokaryotic abundance (PN) or chlorophyll *a* concentration (Chl *a*)

	Prokaryotic abundance		Chlorophyll *a*	
	R^2 (*n*)	*p*	R^2 (*n*)	*p*
Total	0.17 (254)	<0.001	0.21 (208)	<0.001
FRUELA 95	— (115)	0.06	0.13 (86)	0.001
FRUELA 96	0.31 (139)	<0.001	0.22 (122)	<0.001
Drake	0.17 (74)	<0.001	0.16 (61)	<0.001
Bransfield	— (109)	0.057	— (82)	0.124
Gerlache				
Total	0.30 (155)	<0.001	0.18 (113)	<0.001
FRUELA 95	— (69)	0.09	0.22 (38)	<0.001
FRUELA 96	0.44 (84)	<0.001	0.23 (53)	<0.001

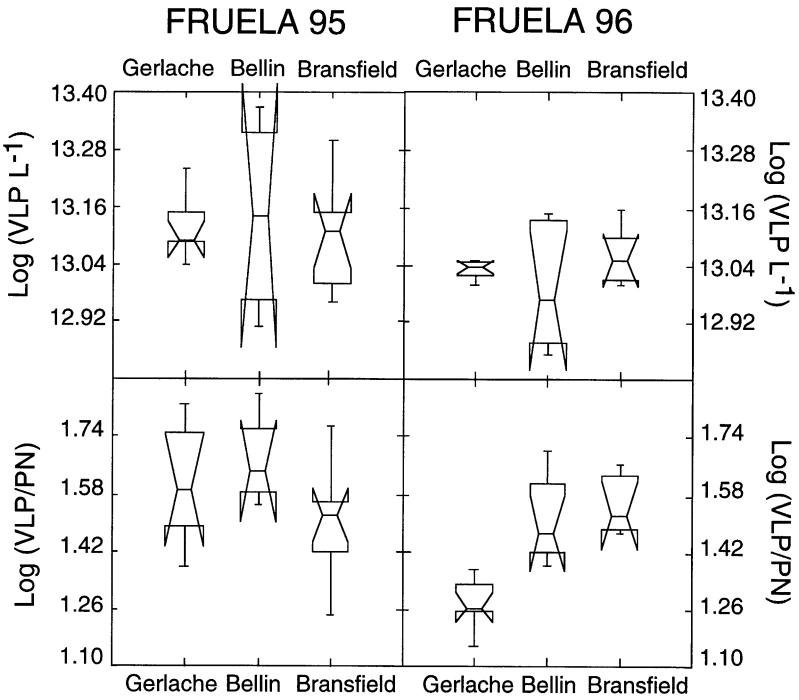

Fig. 3. Integrated values (from the surface to 80–100 m) of log-transformed VLP abundance (Log VLP l^{-1}) and log-transformed VLP/PN ratio (Log VLP/PN) for the three areas studied in each cruise (FRUELA 95 and 96). Box and whiskers graphs are used: The central horizontal line in each box represents the median of the distribution, whereas the other two horizontal lines contain 50% of the values between them. The endpoints of the inclined straight lines indicate the 95% confidence intervals for the median, whereas the whiskers indicate the total range of values without outliers (asterisks; defined as those values greater than 1.5 times the 95% confidence interval for the median).

FRUELA 95 we also found significant differences in the VLP/BN ratio ($p = 0.037$, $n = 20$). A post hoc Tukey test revealed that the significant differences were those between Bellingshausen Sea and Bransfield Strait ($p = 0.037$; Fig. 3).

Seasonal distributions of VLP abundance and the ratio VLP/BN for each area also were checked. Significant differences in the integrated VLP abundance were found only in Gerlache Strait when comparing both cruises ($p < 0.001$). Differences in the VLP/BN ratio were found between FRUELA 95 and 96 in Gerlache Strait ($p < 0.001$, $n = 15$) and in the Bellingshausen Sea ($p = 0.04$, $n = 12$). Values were higher in FRUELA 95 than in FRUELA 96 (Fig. 3).

Diel cycles of VLP abundance were followed in two stations from Gerlache Strait (156 and 169) and one station from Bransfield Strait (168). In all the stations, very slight variations in VLP abundance were found along the day (Fig. 4). In stations 168 and 169 there was a similar pattern, with a maximum of VLP abundance at the beginning and at the end of the cycle (at 10 m depth in station 168, and at 20 m in station 169) and a minimum around noon at the same depths (Figs. 4B and C). The maximal changes in VLP abundance took place in the photic layer. In station 156, the depth distribution of VLP abundance was similar but the maximum occurred at 6:00 h and the minimum at 18:00 h (Fig. 4A). In the rest of the depths VLP abundance changed very little during the day.

3.2. Type I viral decay rate experiments

Changes in VLP abundance with time for the active cultures are shown in Fig. 5. In the experiments carried out at stations 15 and 169,

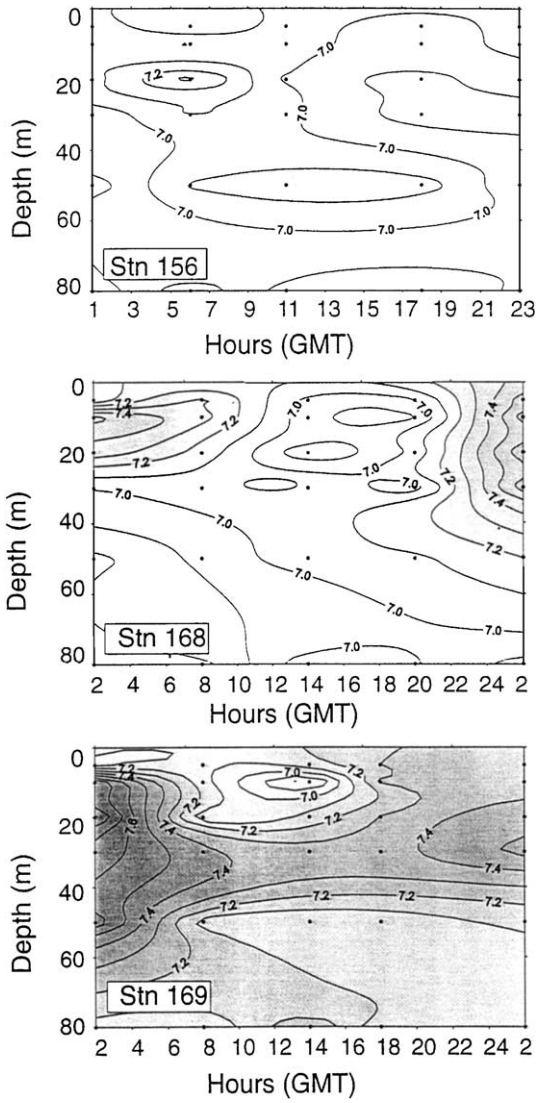

Fig. 4. Diel changes in VLP abundance (log-transformed data) at stations 156 (upper panel), 168 (middle panel) and 169 (lower panel). Filled circles indicate the sampling depths.

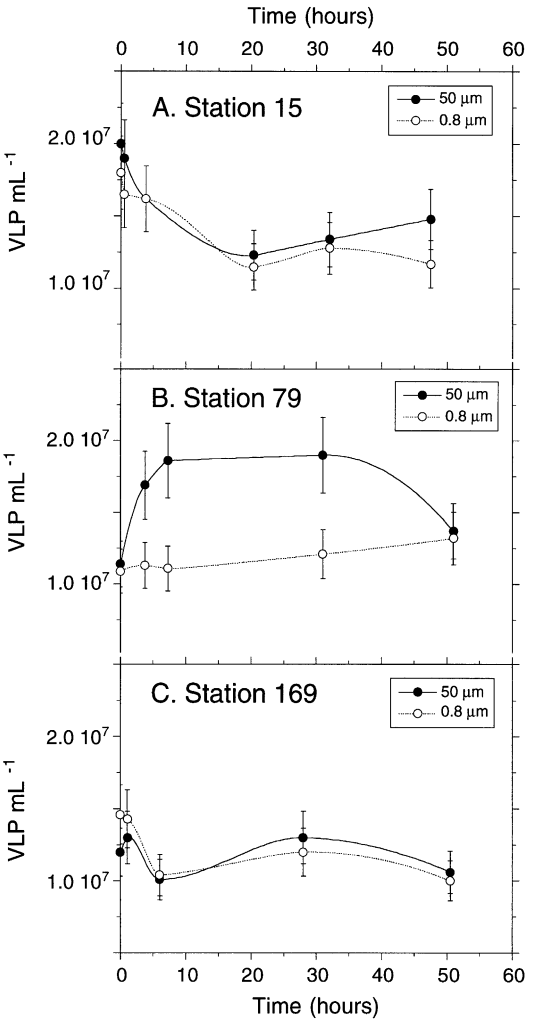

Fig. 5. Changes in VLP abundance (VLP ml^{-1}) in the active cultures from type I decay rate experiments performed at stations 15 (A), 79 (B) and 169 (C). Error bars indicate the average standard error calculated as percentage of the mean from the first sample (3 replicates) in each experiment. Filled symbols indicate samples filtered through 50 µm mesh. Empty symbols indicate samples filtered through 0.8 µm filters.

VLP abundance in the active cultures showed slight changes over the 48 h that the experiments lasted (Figs. 5A and C). In the experiment at station 79, viral abundance at the $<50\,\mu m$ size fraction, increased slightly (less than twice) during the first 10 h of the experiment.

The VLP changes with time for the inactive cultures appear in Fig. 6. In general, the same decay pattern was observed in all the experiments, with a fast decrease in VLP numbers during the first 3–8 h (Figs. 6A–F). After 3–8 h this decrease slowed down, leading to a second rate of decay (Figs. 6A–E). Thus, two different viral decay rates (VDR 1 and VDR 2) were calculated for each experimental bottle (Table 3). VDR 1 corresponded to the first 3–8 h of the experiment.

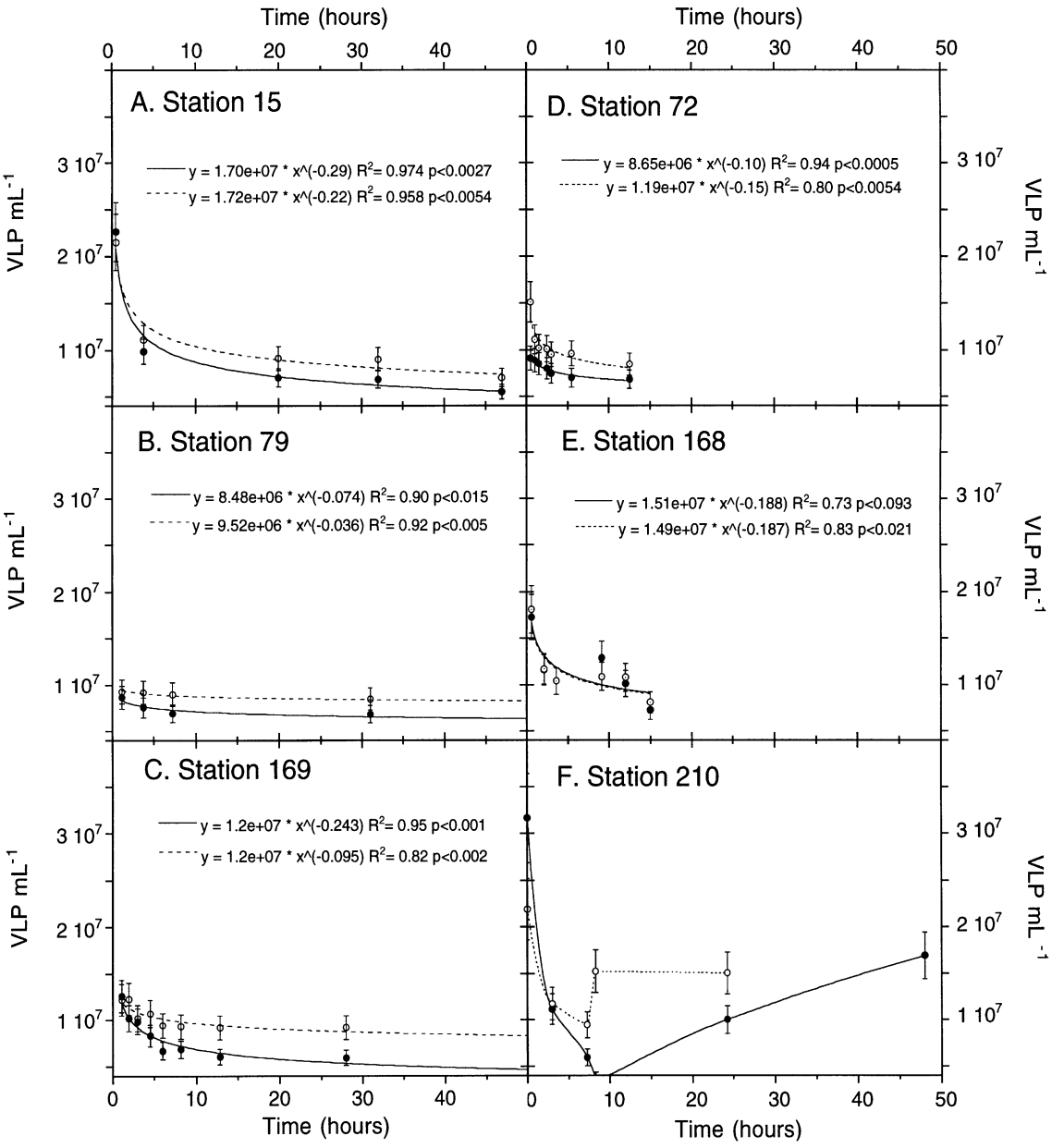

Fig. 6. Changes in VLP abundance in the inactive cultures from type I experiments fitted by a power function (except for station 210) for both size fractions: $<50\,\mu m$ (filled symbols) and $<0.8\,\mu m$ (empty symbols) for stations 15 (A), 79 (B), 169 (C), 72 (D), 168 (E) and 210 (F). Error bars indicate the average standard error calculated as percentage of the mean from the first sample (3 replicates) in each experiment.

VDR 2 was calculated from 3 to 8 h to the end of the experiment. In some cases, rates were not significantly different from 0 ($p > 0.05$; Table 3). In the experiments performed in FRUELA 96 (stations 193 and 210), only VDR 1 could be calculated from the first 3–6 h of the experiment (Table 3; Fig. 6F). The VLP followed an erratic course afterwards apparently caused by the loss of

Table 3
Viral decay rates (VDR) calculated for the first or the second parts of the decay curves, shown in Fig. 6. VDR that are not significantly different from zero are shown in italics

Station	Fraction[a]	VDR (h^{-1})	SE[b]	p	R^2	n[c]	Hours[d]
A. VDR 1							
15	50	*0.208*	0.054	0.162	0.94	3	<4
15	0.8	*0.152*	0.062	0.247	0.86	3	<4
210	50	0.235	0.032	0.017	0.96	4	<8
210	0.8	*0.111*	0.043	0.230	0.87	3	<8
72	50	0.074	0.007	0.002	0.97	5	<3
72	0.8	0.114	0.026	0.021	0.87	6	<3
169	50	0.122	0.048	0.001	0.95	6	<6
169	0.8	0.066	0.014	0.001	0.85	6	<6
193	50	0.260				2	<4
193	0.8	0.207				2	<4
79	50	0.036	0.001	0.022	0.96	3	<8
79	0.8	*0.006*	0.001	0.055	0.99	3	<8
168	50	*0.308*	0.034	0.071	0.99	3	<4
168	0.8	0.173	0.035	0.039	0.92	4	<4
B. VDR 2							
15	50	0.0126	0.0022	0.029	0.94	4	4–48
15	0.8	0.0099	0.0018	0.030	0.94	4	4–48
72	50	*0.0080*	0.0052	0.367	0.70	3	3–15
72	0.8	*0.0139*	0.0047	0.207	0.89	3	3–15
169	50	0.0070	0.0018	0.031	0.83	5	6–48
169	0.8	0.0021	0.0004	0.027	0.94	4	6–48
79	50	*0.0020*	0.0010	0.300	0.80	3	8–48
79	0.8	0.0023	0.0001	0.042	0.99	3	8–48
168	50	0.0950	0.0087	0.056	0.99	3	8–15
168	0.8	*0.0500*	0.0270	0.315	0.75	3	8–15

[a] Cultures filtered through 50-μm mesh or 0.8-μm polycarbonate filters.
[b] Standard error of the slope of the regression.
[c] Number of points used in the regression.
[d] Number of hours used in the regression.

effectiveness of KCN after 24 h. An ANCOVA was used to compare VDR (1 and 2) for both size fractions in each experiment. Although the rates were slightly higher in the <50 μm size fraction in all the stations except for station 72 (Figs. 7A and B), these differences were significant only for station 169 ($p = 0.021$, $n = 12$, for VDR 1 and $p = 0.062$, $n = 9$, for VDR 2).

The overall viral decay rate for each experiment could be fitted by a power function (Figs. 6A–E). When such power functions for both size fractions were compared, the ANCOVA revealed significant differences for the experiments from station 169 ($n = 17$, $p<0.001$) and marginally significant differences for station 79 ($n = 10$, $p = 0.057$). These power functions will be used in the last section.

3.3. *Influence of temperature and glucose addition on viral activity: type II experiments*

Decay patterns for all the experiments incubated at different temperatures were similar (two examples are shown in Figs. 8A and B). VLP abundance decreased at a constant rate from the beginning to 10–25 h, depending on the experiment. Thus, in these experiments only one VDR was calculated from the log-linear part of the curves, using linear

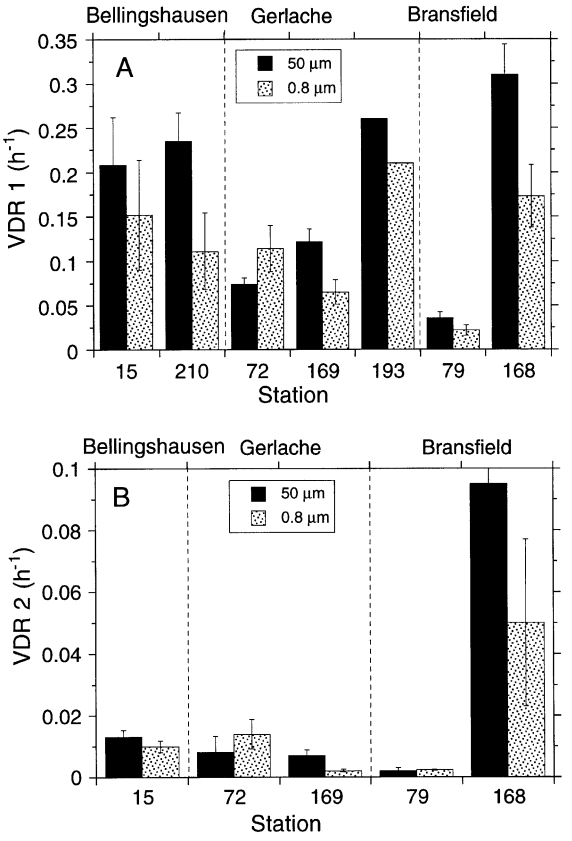

Fig. 7. (A) VDR 1 (viral decay rate from the first hours of type I experiments), for the different stations and for both size fractions (<50 and <0.8 µm). Error bars indicate the standard error of the slope (VDR) of the linear regression. When no error bars are present, VDR has been estimated from two points of the regression line only. (B) VDR 2 (viral decay rate from the later time points of type I experiments) for the different stations and both size fractions (<50 and <0.8 µm). Error bars indicate the standard error of the slope (VDR) of the linear regression.

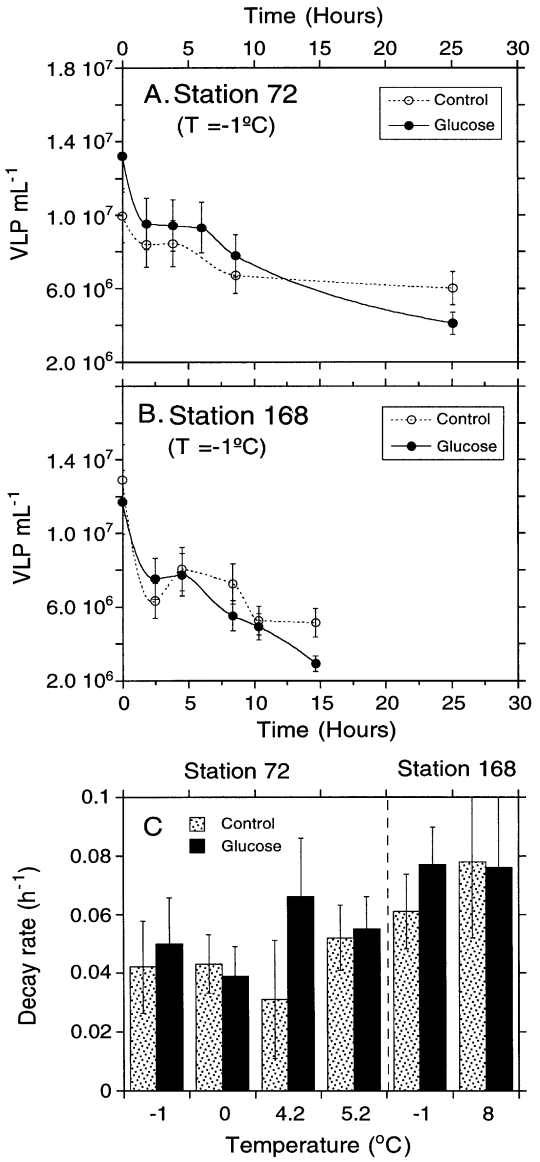

Fig. 8. (A) Decrease in VLP abundance with time in type II decay experiment performed at station 72 at −1°C for both treatments (glucose addition and control). Error bars indicate the average standard error calculated as percentage of the mean from the first sample (3 replicates). (B) Decrease in VLP abundance with time in type II experiment performed at station 168 at −1°C for both treatments (glucose addition and control). Error bars indicate the average standard error calculated as percentage of the mean from the first sample (3 replicates). (C) VDR estimated in type II experiments performed in stations 72 and 168 at different temperatures and for both treatments (glucose addition and control). Error bars indicate the average standard error calculated as percentage of the mean from the first sample (3 replicates) in each experiment.

regression. The resulting VDRs are shown in Fig. 8C, grouped by incubation, temperature and station.

In most cases no significant effects of either temperature or glucose addition could be detected (Table 4). The only two exceptions were the effect of temperature on the glucose-amended cultures at station 72 and the effect of glucose amendment on the cultures incubated at 4.2°C also in station 72, where the significance was marginal.

Table 4
Effects of temperature and glucose addition on viral decay rates. Results of the ANCOVA

Station	Treatment	ANCOVA	
		n	*p*
A. Glucose addition			
72	Control	20	0.462
72	Glucose	23	0.078
168	Control	12	0.983
168	Glucose	11	0.780
B. Temperature			
72	−1	10	0.989
72	0	10	0.680
72	4.2	11	0.068
72	5.2	9	0.780
168	−1	11	0.326
168	8	11	0.635

3.4. Prokaryotic mortality due to viral infection

In the stations where we performed viral decay experiments with the natural sample filtered through 50 μm, we could calculate the impact of viral infection on prokaryotic abundance and production. We assumed that the rate of viral decay measured was equivalent to the rate of viral production (Heldal and Bratbak, 1991). To convert viral production to percentage of prokaryotic mortality due to viral infection, we assumed a range of burst sizes between 50 and 100 (Bratbak et al., 1990). We calculated the percentage of prokaryotic abundance and production that could be removed by viral lysis in three different ways (Fig. 9).

1. Using VDR 1 (Table 3A) we found that prokaryotic mortality due to viral infection exceeded 100% of the prokaryotic production in all stations (Fig. 9A). The percentage of prokaryotic abundance lysed per hour with this rate of viral production ranged between 1.5% in station 79 and 37% in station 168 (Fig. 9B).

2. Using VDR 2 (Table 3B), viral lysis accounted for more than 100% of prokaryotic heterotrophic production only in station 168. In the remaining stations this percentage ranged between 3% and 50% (Fig. 9C). The rate of bacteria lysed per hour was lower than 0.9%, except for station 168 where it was about 15% (Fig. 9D).

3. A third approach was used to calculate viral impact on the prokaryotic assemblage (except at stations 193 and 210), assuming again that the pattern of viral decay would be similar to the pattern of viral production. We calculated the total number of VLP after 25 h using the power function found for each experiment (considering the exponent of the independent variable as positive; Fig. 6). Then we subtracted from this the number of VLP that were present at the first hour of the experiment, calculated with the same function (Figs. 9E and F). The resultant VLP concentration would be the number of VLP produced during a period of 24 h. According to this approach, viral infection would account for less than 100% of the prokaryotic production in three of the stations (72, 79 and 168) and for more than 100% in the other two. Around 50–60% of the prokaryotic abundance would be lysed by viruses daily at stations 72, 168 and 169. At station 79 this percentage was lower than 10% and in station 15 it was close to 100%.

4. Discussion

4.1. Temporal and spatial distribution of viral abundance

Individual values of VLP abundance, ranged between 1×10^6 and 8×10^7 VLP ml^{-1}. The maximal value was found at the surface in station 169 in Gerlache Strait and the minimal values in the deep layers of the vertical profiles. However, 90% of the viral counts were between 7×10^6 and 2×10^7 ml^{-1}. It is difficult to compare these values with those from other studies because in most of them VLP abundance was measured with transmission electron microscopy (TEM). It has been shown that counting YOPRO stained viruses with fluorescence microscopy gives higher estimates of VLP abundance than those obtained with TEM (Hennes and Suttle, 1995; Weinbauer and Suttle, 1997). In order to be able to compare our data

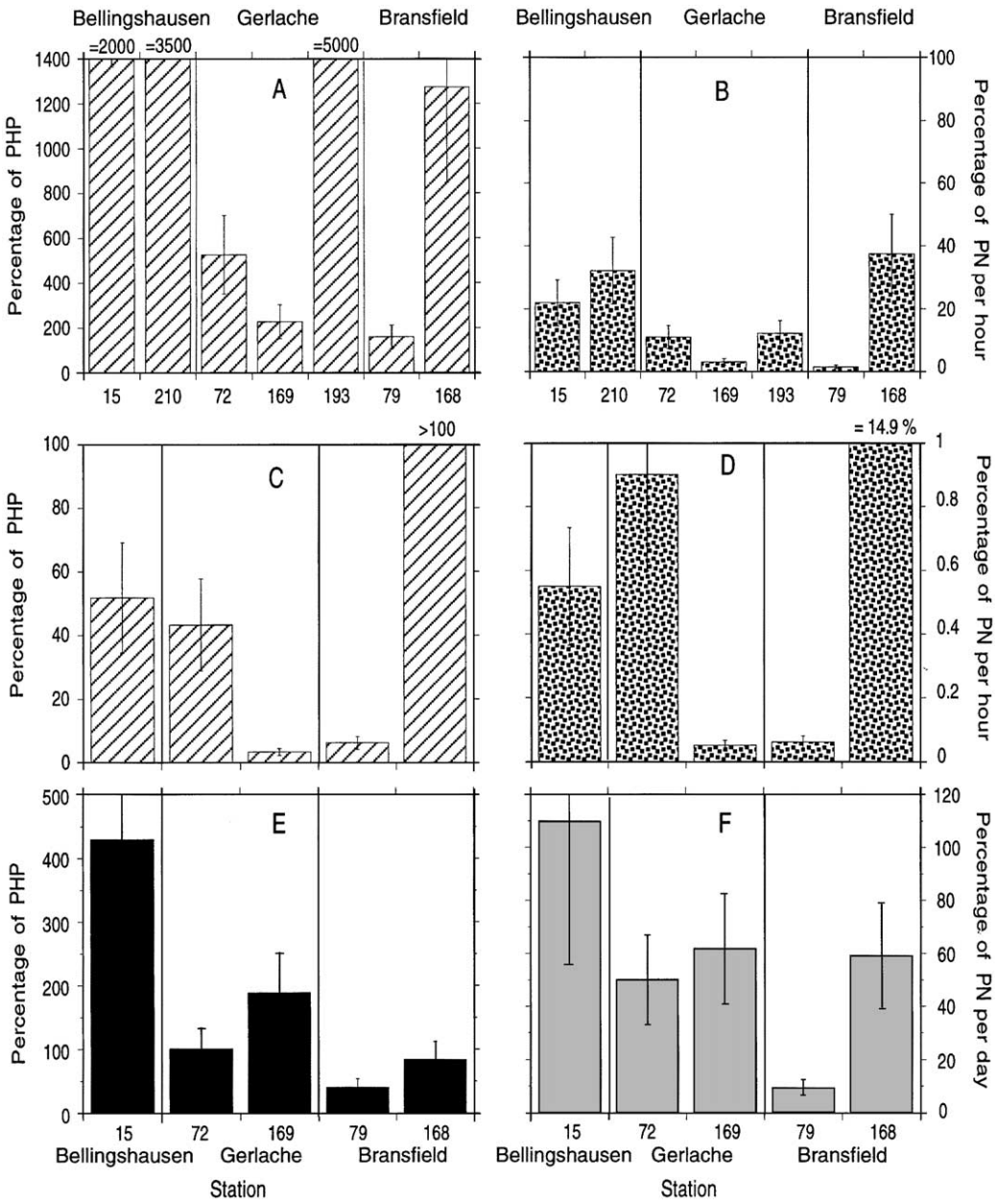

Fig. 9. Percentage of prokaryotic heterotrophic production (PHP) and abundance (PN) lysed by viruses per hour (or day) in different stations according to VDR 1 (A,B), to VDR 2 (C,D) and to the power function (E,F). Error bars indicate the range of values calculated using a range of burst sizes (50–100).

with those from other studies, we transformed our VLP-YOPRO counts to VLP-TEM counts, using a relationship (Log VLP-YOPRO = −0.32 + 1.1Log VLP-TEM) found between the two methods (Guixa-Boixereu et al., 1999b). The transformed values ranged between 5.5×10^5 and 3×10^7 VLP ml^{-1}. This range is much wider than that observed in a previous study of the Belling-

shausen Sea (Smith et al., 1992) and is similar to the range of VLP abundance found by Steward et al. (1996) in the Arctic. However, as we pointed out before, a large percentage of samples showed a range of values smaller than an order of magnitude.

A general trend for lower VLP abundances in FRUELA 96 than in FRUELA 95 was apparent in the three regions. Due to the variability within each region, however, only the values for Gerlache Strait were significantly different. There were no significant differences in VLP among the three zones in either cruise. Taking all data together, variability in VLP abundance was relatively low. No significant relationships were found either with prokaryotic abundance or with chlorophyll *a*. Only when the Gerlache Strait data were considered alone was a significant relationship found between VLP and prokaryotic abundance. The latter variable explained about 50% of the variability of the former.

Small-scale variability was investigated in vertical profiles and diel cycles. Both stations where we analysed deep vertical profiles presented similar patterns of VLP and prokaryotic abundance, with the highest concentrations of both at the surface. In both stations, VLP abundance showed a faster decrease with depth than prokaryotic abundance for the first 30 m. From the surface to this depth, VLP abundance followed the decreasing pattern of chlorophyll *a*. The VLP/BN ratio also decreased with depth. This might indicate that part of the viruses at the surface were phytoplankton viruses. The vertical profile reported by Hara et al. (1996) in a station of the subartic also showed the maximal viral concentrations in the photic zone. However the VLP/BN ratio fluctuated throughout the water column. The one order-of-magnitude decrease in VLP together with the decrease in the VLP/BN ratio with depth would suggest a lower activity of viruses in the deep layers. This is consistent with the lower prokaryotic activity at depth.

Diel cycles of VLP abundance showed, in general, very slight variability. However, in stations 168 and 169 the largest changes occurred at the surface (0–20 m) and the maximal VLP abundance was found at night (2:00), coincident with the minimal solar radiation. This could be due to inhibition of viral activity by sunlight (Suttle and Chen, 1992; Noble and Fuhrman, 1997). In a very dynamic system such as the surface waters of the Gerlache Strait, this could be reflected in a decrease of VLP abundance. In station 156, the pattern was different, and the minimal VLP abundance was reached 5–6 h after the maximal solar radiation.

4.2. Factors responsible of viral decay

Viral decay has been determined in some marine environments for the whole viral assemblage (Heldal and Bratbak, 1991; Mathias et al., 1995; Noble and Fuhrman, 1997) and with some specific phage–host systems (Suttle and Chen, 1992). The difference between viral decay of infectivity and viral decay of particles should be kept in mind. It has been reported that sunlight is one of the most important factors responsible for loss of viral infectivity (Suttle and Chen, 1992; Noble and Fuhrman, 1997). In the dark, adsorption to heat labile particles has been reported to be the factor responsible for both processes: decay of particles and infectivity (Suttle and Chen, 1992; González and Suttle, 1993; Noble and Fuhrman, 1997). Other factors such as grazing by nanoflagellates have been reported to be quantitatively less important (Suttle and Chen, 1992). Recently, Noble and Fuhrman (1999) demonstrated that viruses are labile and turn over relatively rapidly. They suggested that bioreactive molecules in such extracellular enzymes could be responsible for rapid degradation of viral particles.

The fate of viruses when prokaryotic respiration is inhibited by cyanide is unknown (Heldal and Bratbak, 1991). However, losses of viral particles can be only due to abiotic factors and enzymatic activity that does not require energy. Abiotic factors include adsorption to particles and release of nucleic acids from the viral particle (Heldal and Bratbak, 1991). At the moment the fate of virus particles in natural environments due to exoenzymatic activity has not been quantified and the potential importance of this process is unknown.

4.3. Influence of temperature and organic matter on viral activity

No significant differences were found between treatments (control or glucose addition) incubated at different temperatures. Significant differences between both treatments for each temperature were not found in any station. The fact that significant differences were not found may be due to the method used to measure viral activity. As discussed above, the cyanide method would only measure viral decay due to adsorption to particles, most likely to cells. Thus, we could detect differences in viral activity only if bacteria or other particles were found in different amounts in the batch cultures (filtered by 0.8-μm pore size) from which the viral decay rate experiments were carried out. In the batch cultures, ^{3}H-leucine incorporation started to increase after the second sampling day in the glucose addition treatment incubated at the highest temperatures ($>4^{\circ}C$) and later in the other treatments. Prokaryotic abundance, however, did not increase after the third sampling day (Pedrós-Alió et al., 2002). Thus, we suggest that when decay experiments were performed, changes in prokaryotic abundance were not sufficient to be reflected in significantly higher viral adsorption. Consequently, the cyanide method might have not been sensitive enough to detect differences in viral activity due to either temperature or organic matter addition.

4.4. Prokaryotic mortality due to viral lysis estimated from decay experiments: limitations of the methodology

Viral decay experiments using KCN as inhibitor of biological activity have been used previously to measure viral production rates (Heldal and Bratbak, 1991; Bratbak et al., 1992; Mathias et al., 1995). In this approach it is assumed that the VLP abundance in the system is maintained constant through time. In order to test this assumption, we also incubated active cultures where VLP abundance showed slight fluctuations through time (Fig. 5). Thus, it seems that the viruses lost by decay were actually replaced by viruses released from lysed prokaryotic cells.

The first drawback of the method is that it could underestimate viral decay rates because biotic processes are not considered. Thus, viral production estimated with cyanide would represent, a priori, a conservative approach to the actual viral production in aquatic environments.

Another disadvantage of the method is that an estimate of burst size is needed to transform viral production rate into prokaryotic mortality. A wide range of values of burst sizes from bacteria in natural environments has been found (Weinbauer and Peduzzi, 1994). A lower burst size would mean an overestimation of viral mortality. Steward et al. (1996) found that bacteria from the Arctic contained phages in a range between 6 and 270. However, these authors used an average burst size of 50 to convert the estimates of viral production to prokaryotic mortality. We assumed a range of burst sizes between 50 and 100 as representative of marine bacteria (Bratbak et al., 1990).

All the calculations to convert viral decay rates to prokaryotic mortality have assumed that all VLP were bacteriophages. As pointed out before, an important part of the VLP could be phytoplankton viruses, and thus our prokaryotic mortality values would be overestimates.

The main problem of the cyanide method is the difficult interpretation of viral decay experiments. Curves obtained from these experiments showed a fast rate in the first hours and a slow rate afterwards (24–48 h). This pattern was also found by Heldal and Bratbak (1991) and Mathias et al. (1995). In this situation there are three options: (1) to consider the first rate as valid and the second as an artefact of the incubations; (2) to consider the first as an artefact of enclosing samples in bottles and the second rate as the valid one and (3) to fit a power function to the whole data set and to use this to calculate losses for a given period of time.

1. The first option is the one taken by Heldal and Bratbak (1991) and Mathias et al. (1995). In this case, the assumption is that as the experiment proceeds, all the possible sites for phage adsorption become occupied and therefore the asymptotic part of the curve is not valid for nature. The viral decay rates found during the first hours of the experiments (VDR 1) in Antarctic waters ranged between 0.006 and 0.3 h^{-1}. These values showed a

higher range of variability than those found by Mathias et al. (1995) (0.06–0.1 h^{-1}) in samples from the Danube River. The upper values of our VDR 1 are in the range of rates estimated by Heldal and Bratbak (1991) in a Norwegian fjord.

The prokaryotic mortality necessary to maintain the viral production estimated with VDR 1 was always higher than 100% of the prokaryotic production. The lowest impact of viruses on the prokaryotic assemblage derived from VDR 1 was found at stations 79 and 169 (1–3% of BN per hour). Even assuming that viral lysis was the only factor responsible for prokaryotic mortality in these stations, bacteria would have to grow at a rate twice that found to maintain a constant abundance. This result is difficult to accept because even though values of prokaryotic heterotrophic production could be underestimated (Calderón-Paz, 1997), other causes of prokaryotic mortality were certainly present (Vaqué et al., 2002). At the other stations the imbalance was even worse. Thus, the percentage of prokaryotic mortality due to viral infection obtained with the VDR 1 seems totally unrealistic. This is in agreement with the results found by Bratbak et al. (1990) in a diel mesocosm experiment, where viral lysis exceeded prokaryotic production by a factor of 6. We think that cyanide addition may affect the natural community not just by stopping its activity. Processes favouring formation of aggregates could be involved that would artificially increase the rate of viral decay. In some environments this may not be the case. Thus, Mathias et al. (1995) used two approaches (percentage of infected bacteria and viral decay after cyanide addition) to measure prokaryotic mortality due to viral lysis. The values obtained with both methods overlapped, giving estimates of prokaryotic mortality due to viral infection between 11% and 43% of the whole prokaryotic mortality (assuming balanced prokaryotic growth).

2. In the second approach the assumption is that the initial fast decay is due to the bottle enclosure and only after a few hours is the natural decay rate restored. An alternative interpretation is that at least two "kinds" of viruses with different kinetics of disappearance are present. In fact Mathias et al. (1995) obtained some evidence of this situation. They observed that smaller viruses (<60 nm) showed a faster decay (VDR 1) while larger viruses decreased slowly (VDR 2). Thus, the VDR 2 might correspond to a portion of the initial viral assemblage. Using VDR 2 to calculate prokaryotic mortality due to viral infection gives more realistic results. However, it is not possible to use this rate to measure the whole viral impact on the natural prokaryotic assemblage because the smaller viral particles with a faster decay might be ignored (Mathias et al., 1995).

3. The last approach is more pragmatic. If we assume there are two or more different virus populations with different decay rates, an exponential decrease cannot be expected. The use of the power function found for each experiment to calculate prokaryotic mortality is statistically the most satisfying approach. However, it has two problems. First, long incubations are needed and cyanide seems to decrease its effect after 24 h (see for example Fig. 6F). This could be the reason why in stations 193 and 210, where we did not add cyanide again after 24 h, we did not obtain a clear pattern in the decay experiments. And second, with this approach an exponential viral decay rate cannot be calculated. Still, the total number of viruses produced per day can be calculated as has been explained in Section 3.4. Production and decay take place continuously in nature. To manipulate the natural community by blocking one of these processes for a long period of time may give unrealistic results. Control incubations of active cultures, however, seemed to indicate that net changes of viruses were zero throughout the 48 h that the experiments lasted. Thus, the approach of using the data from the whole decay experiment to estimate prokaryotic mortality seems the most appropriate.

Let us, then, consider the results of prokaryotic mortality due to viral infection derived from the power function. Viral impact on the natural prokaryotic assemblage would account for a significant percentage of production. In station 79, viral lysis accounted for 40% of the prokaryotic production. In stations 72 and 168, viral impact accounted for 100% of the prokaryotic production. In these stations viruses would be responsible for all the prokaryotic losses possible

with the experimentally determined specific growth rates (0.41 and 0.53 d^{-1} respectively). In stations 15 and 169 bacteria should grow at a rate faster than the measured one (twice in station 169 and three times in station 15) to be able to maintain a constant abundance.

In Arctic waters viral infection has been found to account for 10–23% of the prokaryotic heterotrophic production on average (Steward et al., 1996). The highest values reported in the latter study (36%) are equivalent to the lowest values found in the present work. The viral impact found by Steward et al. (1996) was estimated by counting visibly infected bacteria (VIB) in whole cell preparations (Weinbauer and Peduzzi, 1994). It has been reported that this method could underestimate prokaryotic mortality due to viral infection because of the possibility of disruption of cells during ultracentrifugation (Weinbauer and Peduzzi, 1994; Steward et al., 1996) and because some cells that could be infected appear opaque under TEM (Guixa-Boixereu et al., 1999a, b). Moreover, to convert VIB to prokaryotic mortality it is necessary to use a range of conversion factors that have been calculated experimentally only for two marine phage–bacteria host systems by thin sectioning (Proctor et al., 1993). Thus, there are some uncertainties in the method of counting VIB that seem to cause underestimations of viral impact on the prokaryotic assemblage (Steward et al., 1996). As has been pointed out above, the cyanide method also has disadvantages and in some cases it seems to give estimations of viral impact difficult to reconcile in nature (stations 15 and 169 in this study; Heldal and Bratbak, 1991; Bratbak et al., 1992). Thus, more work is needed to improve both methods of estimating prokaryotic mortality due to viruses. For the cyanide method it would be necessary to know the mechanisms involved in the disappearance of viruses observed.

Despite the uncertainties in our estimations of prokaryotic mortality due to viruses, some tentative conclusions appear reasonable. Viral lysis presented the highest impact in the most eutrophic station (15) and the lowest impact in the most oligotrophic station (79). This is in agreement with other studies that found that viral mortality of bacteria was higher in more eutrophic waters (Weinbauer and Peduzzi, 1995; Steward et al., 1996).

When comparing viral lysis and bacterivory at the stations where both processes were measured (Vaqué et al., 2002; Fig. 10), viruses always accounted for a percentage of the prokaryotic production and abundance larger than bacteri-

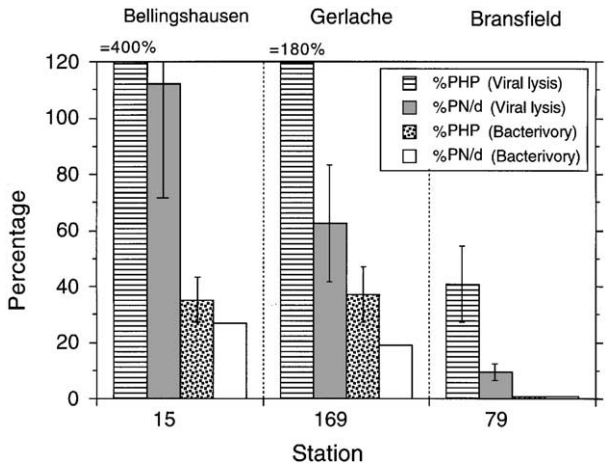

Fig. 10. Percentage of prokaryotic heterotrophic production (PHP) and abundance (PN) ingested by bacterivores and lysed by viruses per day in different stations. Error bars indicate the range of values calculated using a range of burst sizes (50–100). Bacterivory data taken from Vaqué et al., 2002).

vores. This result is different from that presented by Steward et al. (1996) in the Arctic, who found that viral lysis and bacterivory accounted for a similar percentage of prokaryotic mortality (25% each). A differential response of microbial processes to temperature has been suggested to occur in cold waters (e.g., Pomeroy and Deibel, 1986). This feature has been studied for bacterioplankton and phytoplankton. If this characteristic were general, uncoupling could occur between any two trophic links in the microbial food webs. Vaqué et al. (2002) have found extremely low values of bacterivory in Antarctic waters. Bacterivory increased only after prokaryotic abundance and activity were stimulated artificially (Calderón-Paz, 1997). Thus, bacterivory and prokaryotic activity also seem to be uncoupled in cold environments. We could expect viruses to be coupled to prokaryotic activity because they need the cell enzymes to multiply. Thus, in cold environments, viruses could cause a higher impact on prokaryotic mortality than bacterivores, at temperatures where bacterivores show a lower activity than bacteria. Clearly, more work is necessary to test this hypothesis.

Acknowledgements

We thank our fellow scientists during FRUELA, the cruise leaders Ricardo Anadón and Marta Estrada, and the crew of the *BIO Hespérides* for their help during the cruises. The present work was funded by grant ANT94-1010 from CICYT.

References

Bird, D.F., Karl, D.M., 1991. Spatial patterns of glutamate and thymidine assimilation in Bransfield Strait, Antarctica during and following the austral spring bloom. Deep-Sea Research II 38, 1057–1075.

Bratbak, G., Heldal, M., Norland, S., Thingstad, T.F., 1990. Viruses as partners in spring bloom microbial trophodynamics. Applied Environmental Microbiology 56, 1400–1405.

Bratbak, G., Heldal, M., Thingstad, T.F., Riemann, B., Haslund, O.H., 1992. Incorporation of viruses into the budget of microbial C-transfer. A first approach. Marine Ecology Progress Series 83, 273–280.

Calderón-Paz, J.I., 1997. Ecología de las bacterias heterotróficas en ecosistemas planctónicos. Ph.D. Thesis, Universitat de Barcelona, Barcelona, Spain.

Gomis, D., García, M.A., López, O., Pascual, A., 2002. Quasi-geostrophic 3D circulation and mass transport in the western Bransfield strait during austral summer 1995/96. Deep-Sea Research II 49, 603–621.

González, J.M., Suttle, C.T., 1993. Grazing by marine nanoflagellates on viruses and viral-sized particles: ingestion and digestion. Marine Ecology Progress Series 94, 1–10.

Guixa-Boixereu, N., Lysnes, K., Pedrós-Alió, C., 1999a. Viral lysis and bacterivory during a phytoplankton bloom in a coastal water microcosm. Applied Environmental Microbiology 65, 1949–1958.

Guixa-Boixereu, N., Calderón-Paz, J.I., Gasol, J.M., Pedrós-Alió, C., 1999b. Distribution of viruses and their potential effect on bacterioplankton in an oligotrophic marine system. Aquatic Microbial Ecology 19, 205–213.

Hara, S., Koike, I., Terauchi, K., Kamiya, H., Tanque, E., 1996. Abundance of viruses in deep oceanic waters. Marine Ecology Progress Series 145, 269–277.

Heldal, M., Bratbak, G., 1991. Production and decay of viruses in aquatic environments. Marine Ecology Progress Series 72, 205–212.

Hennes, K.P., Suttle, C.T., 1995. Direct counts of viruses in natural waters and laboratory cultures by epifluorescence microscopy. Limnology and Oceanography 40, 1050–1055.

Karl, D.M., 1993. Microbial processes in the southern ocean. In: Friedman, E.I. (Ed.), Antarctic Microbiology. Wiley, New York, pp. 1–63.

Kirchman, D.L., K'Nees, E., Hodson, R.E., 1985. Leucine incorporation and its potential as a measure of protein synthesis by bacteria in natural aquatic systems. Applied Environmental Microbiology 49, 599–607.

Maranger, R., Bird, D.F., 1995. Viral abundances in aquatic systems: a comparison between marine and fresh waters. Marine Ecology Progress Series 121, 217–226.

Maranger, R., Bird, D.F., Juniper, S.K., 1994. Viral and bacterial dynamics in Arctic sea ice during the spring bloom near resolute, N.W.T., Canada. Marine Ecology Progress Series 111, 121–127.

Mathias, C.B., Kirschner, A.K.T., Velimirov, B., 1995. Seasonal variations of virus abundance and viral control of the bacterial population in backwater system of the Danube river. Applied Environmental Microbiology 61, 3734–3740.

Noble, R.T., Fuhrman, J.A., 1997. Virus decay and its causes in coastal waters. Applied Environmental Microbiology 63, 77–83.

Noble, R.T., Fuhrman, J.A., 1999. Breakdown and microbial uptake of marine viruses and other lysis products. Aquatic Microbial Ecology 20, 1–11.

Norland, S., Heldal, M., Tumyr, O., 1987. On the relation between dry matter and volume of bacteria. Microbial Ecology 13, 95–101.

Pedrós-Alió, C., Vaqué, D., Guixa-Boixereu, N., Gasol, J.M., 2002. Prokaryotic plankton biomass and heterotrophic production in western Antarctic waters during the 1995–96 Austral summer. Deep-Sea Research II 49, 805–825.

Pomeroy, L.R., Deibel, D., 1986. Temperature regulation of bacterial activity during the spring bloom of Newfoundland coastal waters. Science 233, 359–361.

Porter, K.G., Feig, Y.S., 1980. The use of DAPI for identification and enumeration of bacteria and blue–green algae. Limnology and Oceanography 25, 943–948.

Proctor, L.M., Fuhrman, J.A., 1990. Viral mortality of marine bacteria and cyanobacteria. Nature 343, 60–62.

Proctor, L.M., Okubo, A., Fukrman, J.A., 1993. Calibrating estimates of phase-induced mortality in marine bacteria: ultrastructural studies of marine bacteriophage development from one-step growth experiments. Microbial Ecology 25, 161–182.

Smith, D.C., Azam, F., 1992. A simple economical method for measuring bacterial protein synthesis rates in seawater using ^{3}H-leucine. Marine Microbial Food Webs 6, 107–114.

Smith, D.C., Steward, G.F., Azam, F., Hollibaugh, J.T., 1992. Virus and bacteria in the Bellingshausen Sea during January and August 1991. Antarctic Journal US 27, 125–127.

Steward, G.F., Wikner, J., Cochlan, W.P., Smith, D.C., Azam, F., 1992. Estimation of virus production in the sea: II. Field results. Marine Microbial Food Webs 6, 79–90.

Steward, G.F., Smith, D.C., Azam, F., 1996. Abundance and production of bacteria and viruses in the Bering and Chukchi Seas. Marine Ecology Progress Series 131, 287–300.

Suttle, C.T., Chen, F., 1992. Mechanisms and rates of decay of marine viruses in seawater. Applied Environmental Microbiology 58, 3721–3729.

Vaqué, D., Guixa-Boixereu, N., Pedrós-Alió, C., Gasol, J.M., 2002. Distribution of microbial biomass and importance of protests in regulating prokaryotic assemblages in three areas close to the Antarctic Peninsula in spring and summer 1995–96. Deep-Sea Research II 49, 847–867.

Weinbauer, M.G., Peduzzi, P., 1994. Frequency, size and distribution of bacteriophages in different marine bacterial morphotypes. Marine Ecology Progress Series 108, 11–20.

Weinbauer, M.G., Peduzzi, P., 1995. Significance of viruses versus heterotrophic nanoflagellates for controlling bacterial abundance in the Northern Adriatic Sea. Journal of Plankton Research 17, 1851–1856.

Weinbauer, M.G., Suttle, C.T., 1997. Comparison of epifluorescence and transmission electron microscopy for counting viruses in natural marine waters. Aquatic Microbial Ecology 13, 225–232.

Yentsch, C.S., Menzel, D.W., 1963. A method for determination of phytoplankton chlorophyll and phaeophytin by fluorescence. Deep-Sea Research 10, 221–231.